DFTB approach to multiply charged Aunq+ clusters

Nathalie Tarrat, Mathias Rapacioli, Bishal Poudel, Fernand Spiegelman

▶ **To cite this version:**

Nathalie Tarrat, Mathias Rapacioli, Bishal Poudel, Fernand Spiegelman. DFTB approach to multiply charged Aunq+ clusters. Journal of Innovative Materials in Extreme Conditions, 2024, 5 (2), pp.115. hal-04737008

HAL Id: hal-04737008
https://hal.science/hal-04737008v1

Submitted on 15 Oct 2024

HAL is a multi-disciplinary open access archive for the deposit and dissemination of scientific research documents, whether they are published or not. The documents may come from teaching and research institutions in France or abroad, or from public or private research centers.

L'archive ouverte pluridisciplinaire **HAL**, est destinée au dépôt et à la diffusion de documents scientifiques de niveau recherche, publiés ou non, émanant des établissements d'enseignement et de recherche français ou étrangers, des laboratoires publics ou privés.

Distributed under a Creative Commons Attribution 4.0 International License

Journal of Innovative Materials in Extreme Conditions
2024
Volume 5
Issue 2

DFTB APPROACH TO MULTIPLY CHARGED Au^{q+}_n CLUSTERS PART II-ENERGETICS, FRAGMENTATION AND IONIZATION

Nathalie Tarrat [1,a], Mathias Rapacioli [2,b], Bishal Poudel[2], Fernand Spiegelman[2]

[1] *CEMES, CNRS, Universit´e de Toulouse, 29 Rue Jeanne Marvig, 31055 Toulouse, France*
[2] *Laboratoire de Chimie et Physique Quantiques LCPQ/FeRMI, UMR 5626, Universit´e de Toulouse (UPS) and CNRS, 118 Route de Narbonne, F-31062 Toulouse, France*

Corresponding author: [a] nathalie.tarrat@cemes.fr; [b] rapacioli@irsamc.ups-tlse.fr

[$] Dedicated to J. Christian Schön on the occasion of his 66th birthday

Abstract: *This article corresponds to part II of a series about singly and multiply charged gold clusters. From their total energies in the size range n = 3 − 20 and charge q = 0 − 4 determined in part I one of the series, it aims to present a Density Functional based Tight Binding approach of their stability/metastability versus atomization and fragmentation, as well as their ionization properties to different charge states. The present DFTB results are discussed with respect to previous theoretical or experimental investigations.*

Keywords: *gold clusters, charge, stability, fragmentation, ionization*

1. Introduction

The energetical properties of clusters (possibly singly or multiply charged) have fostered a variety of studies related to their stability, fragmentation, and ionization properties (see for instance textbooks [1-4]). Numerous theoretical studies based on structure determination are available for neutral and singly ionized gold clusters on a wide range of sizes (see for instance recent papers [5-11] and references therein). However, since the finding that even doubly or triply charged clusters as small as Au^{2+}_2 and Au^{3+}_4 could be observed with a finite lifetime [12-13], various experimental studies have also investigated fragmentation properties of multiply charged gold clusters following either laser or collisional energy deposit [14-23]. Most of the results have been interpreted with the help of the liquid drop model [24-28] while only very partial atomistic studies are available [29-33]. The present article features part II of a theoretical work on multiply charged gold clusters Au^{q+}_n, their global structures and energies in the size range n = 3 − 20 and charge range q = 0 − 4 having been determined and discussed in part I of the series. It was found that, within the DFTB approach, global minima could be obtained from the ground state potential energy surface exploration (PES), for all sizes up to charge +2 for sizes from 4 for charge +3, and from 6 for charge +4. In the present part II, we will discuss the stability properties of clusters, their fragmentation channels according to energetical criteria, and their ionization properties.

2. Cohesive energies and stability

We first discuss the stability in terms of cohesive energies. In the case of multiply charged clusters, cohesive cluster charge, and geometrical structure are mostly coupled (ii) determine the energetical properties, such as stability, metastability, ionization, and fragmentation properties (iii) probe whether energies can be defined in several ways. We take here the definition of the cohesive energy per atom e_c as corresponding to atomization into neutral atoms and singly charged atomic ions only

$$e_c(n,q) = -[E_n^{q+} - (n-q)E_1^0 - qE_1^+]/n \quad (1)$$

with E^{q+}_n being the total energy of a cluster of size *n* and charge +*q*. This chosen reference atomization energy is the lowest one. Figure 1 and Table I show the evolution of the cohesive energies for different charge states. The cohesive energies for neutrals and monocations are always positive, which is no longer the case for tri- and tetra-cations. Au^{2+}_2 has a very weak metastable well at 3.76 eV above dissociation in Au^++Au^+, in agreement with the DFT calculation by Ortiz et al. [30], while further studies [29-34] find it essentially repulsive with a flat range around R = 2.6 − 2.8 Å. While no minimum was found on the PES below n=4 for tri-cations and n=6 for tetra-cations, positive cohesive energies vs atomization are found at n = 6 for Au^{3+}_n and n = 8 only for Au^{4+}_n . This means that below those critical sizes, all isomers are metastable even when they exist on the PES. This does not preclude metastability up to larger sizes with respect to other dissociative channels as will be discussed in section III. It can be seen in Figure 1 that the cohesive energies of all charge species increase with size, expectedly converging to the bulk asymptotic DFTB value e^{bulk}_c =2.889 eV [35]. The convergence is slower for the higher-charged species. Obviously, size effects are present in the relative stabilities and can be better evidenced in Figure 2 where the second difference of the energy with respect to size

$$\Delta_2(n) = E(n+1) - 2E(n) + E(n-1) \quad (2)$$

are shown. As expected and already discussed in a number of studies [5, 10, 36-41] in the case Au_n and Au^+_n , the second differences show an odd-even alternation, the even sizes being more stable in the case of neutrals, and conversely for singly charged clusters [38]. This corresponds to enhanced stability when the HOMO orbital is filled with a pair of electrons.

n	Au_n	Au_n^+	Au_n^{2+}	Au_n^{3+}	Au_n^{4+}
2	1.560	1.269	-1.882	-	-
3	1.627	2.190	0.071	-	-
4	2.032	2.227	1.221	-1.200	-
5	2.191	2.456	1.585	-0.047	-
6	2.466	2.532	1.993	0.633	-1.076
7	2.411	2.681	2.155	1.174	-0.274
8	2.543	2.699	2.376	1.474	0.314
9	2.537	2.838	2.472	1.755	0.729
10	2.624	2.792	2.688	1.923	1.095
11	2.632	2.856	2.652	2.123	1.332
12	2.713	2.838	2.746	2.222	1.550
13	2.713	2.886	2.730	2.350	1.684
14	2.782	2.883	2.801	2.398	1.817
15	2.781	2.925	2.818	2.530	1.942
16	2.810	2.928	2.853	2.530	2.046
17	2.829	2.977	2.853	2.608	2.117
18	2.873	2.973	2.907	2.625	2.253
19	2.894	3.008	2.912	2.686	2.247
20	2.949	3.015	2.943	2.692	2.332

Table I. Cohesive energies per atom (in eV) of Au^{q+}_n clustersfor atomization into (n −q)Au+qAu^+.

Other special stabilities can be seen in the case of neutrals at 2 and 6, and in the case of monocations at 3 and 9. Those special sizes have been interpreted in terms of shell closures in the 2D (2 or 6 electrons) and

3D spherical shell models (2 or 8 electrons), respectively. Interestingly, the odd-even stability alternation is also observed for di- and tri-cations, and even for tetra-cations with the exception of a missing positive peak at n=14. Enhanced stabilities are also significant for Au^{2+}_4 , Au^{2+}_{10} (8 electrons within a 3D structure with T_d symmetry, also evidenced with DFT by Petrar et al. [33]), Au^{2+}_{12} , Au^{3+}_{15} and Au^{4+}_{18} . The shift of the stability maxima with charge thus seems somehow correlated with the effective number of electrons.

3. Fragmentation

The energetical aspects of fragmentation in multiply charged clusters have been widely documented [12, 14, 15, 26-28, 42]. Energetically, fragmentation is governed by the following factors: (i) the bonding, (ii) the occurrence of Coulomb fragmentation barriers, (iii) the energy balance of the fragmentation channels, and (iv) the dynamical and entropic effects, less documented. Theoretical approaches in the case of gold clusters have been carried out in the framework of the deformed liquid drop model [26-28, 42], possibly including quantum aspects within a jellium description. Working within an atomistic framework is obviously a challenge if one considers fragmentation barriers of an ionized/multiply ionized cluster into all possible charge/size dissociation channels on a complex multi-dimensional PES. We only provide and discuss here the energy balance between the lowest energy isomers and their lowest energy fragmentation channels.

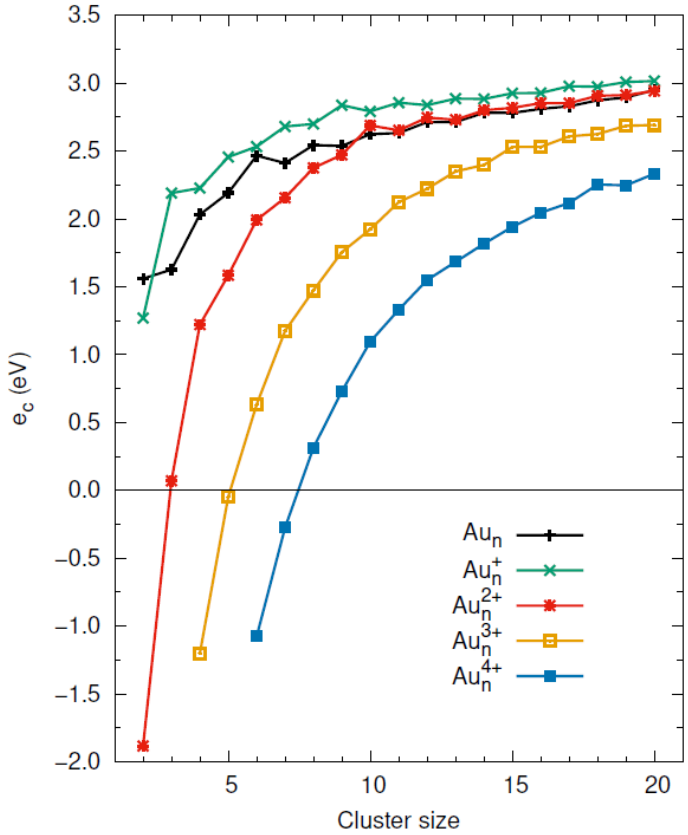

Figure 1. Cohesive energies per atom of Au^{q+}_n clusters for atomization into (n − q)Au+qAu^+.

Table II provides the energies E_{lfc} of the lowest fragmentation channels observed from our DFTB calculations (all channels have been scanned, including three- and four-fragment fragmentation paths which actually never appear as the most favorable energetically). In addition, the channels corresponding to the evaporation of a single neutral monomer ($\Delta 1$) are also reported, as well as those corresponding to the evaporation of a dimer ($\Delta 2$) relevant for the cases q = 0, 1. It should be stressed that the relationship of these data to the experiments is only partial since Coulomb fission barriers are not included in the balance, while they are certainly an essential feature in the case of multiply charged clusters. In the case of neutral and singly charged clusters, the lowest energy dissociation channels essentially correspond to the evaporation of a monomer or of a dimer. For neutrals, dimer evaporation is favored for even sizes, while monomer evaporation is favored in odd cases. A noticeable exception occurs for Au_{12} where dissociation into two stable Au_6 moieties is energetically favored. The odd-even alternation breaks down at n = 16, beyond which monomer fragmentation becomes systematic. The odd-even rule is reversed in the case of Au^+_n clusters where monomer evaporation is found as the lowest channel for even sizes while dimer evaporation is the lowest for odd sizes, the charge being always carried by the largest fragment. Those results for Au^+_n are in general agreement with the laser-induced fragmentation experiments in traps [16, 18-21, 43, 44]. Note that monomer evaporation tends to take over in some experiments [43] for n > 14, while the alternation persists in our results with however a $|\Delta 1-\Delta 2|$ difference of less than ~ 0.25 eV for n =15, 17, and 19. Also, the present DFTB theoretical decay energies into a dimer are 3.74, 2.76, 2.97, and 3.23 for sizes n =9, 11, 13, and 15 respectively with DFTB to be compared with experimentally measured dissociation energies 3.66, 4.27, 4.29 and 4.29 eV, apparently showing theoretical underestimation for the last three values. In the case of Au^{2+}_n clusters, Table II shows that only clusters with sizes $n \geq 8$ have positive DFTB dissociation energies and are absolutely stable versus fragmentation. Actually, the critical size for the stability of doubly charged gold clusters was established at n = 9 with gas aggregation techniques [45]. This number is however strongly dependent upon the experimental conditions, indeed fragmentation of Au^{2+}_7 could be investigated in Penning traps [22]. Table II further shows that the loss of a charged trimer is the preferential channel in the fragmentation of small doubly charged clusters. Those results are in general agreement with experimental collision-induced fragmentation studies [22-42]. Exceptions in the present results can be found for n = 10 and 19 where monomer dissociation is favored, and for sizes n = 15 − 18 which might energetically undergo more symmetric fission, one favored fragmentation product being Au^{+9} which was mentioned above as particularly stable. From the present study, Au^{3+}_n and Au^{4+}_n are only metastable versus fragmentation, with negative dissociation energies. The critical size for the stability of Au^{3+}_n was estimated at n = 22, which is slightly beyond the sizes investigated here. Collision-induced fragmentation patterns for triply charged gold clusters were published by Ziegler et al. [22] for sizes n > 19 at the limit of those investigated in the present work, showing a preference for asymmetric fission into a trimer ion for sizes in between 19 and 27 and a competition with neutral monomer evaporation for larger sizes. The present results show that the small clusters, if they could be stabilized experimentally might undergo fission into $Au^{2+}_{n-1}+Au^+$ below n=11. For n > 11, there is a stronger competition, the large fragment remaining always doubly charged while preference for fission into $Au^{2+}_{n-3}+Au^+_3$ occurs frequently in the size range 13-20. Finally, in the case of Au^{4+}_n, the lowest energy channels always contain either fragments Au^{2+}_4 or Au^{2+}_{10}, which is in line with the large stabilities of those fragment clusters. The only exception is observed for size n = 12 in which case the fission channel into two Au^{2+}_6 is the lowest one.

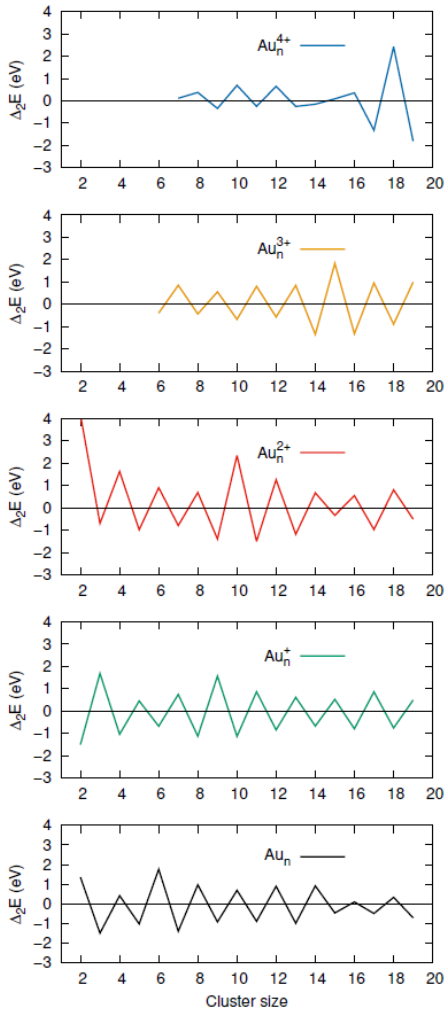

Figure 2. Second derivatives $\Delta_2 E$ of the total energies of gold clusters Au^{q+}_n with n = 2 − 19 and q = 0 − 4.

4. Ionization properties

As was found in the paper I, the geometries of the ground state isomers start to strongly deviate from those of the neutrals for n > 2. Hence, we first show in Table III the vertical total ionization energies of the clusters above the most stable neutral isomer. The first observation is that, except in the case of the first one (ionization towards Au+n), the ionization energies all undergo strong drops by about 5, 12, and 25 eV respectively between n = 1 and n = 2. If we now look at the adiabatic ionization potentials, namely the difference shown in Figure 3 and listed in Table III, the drop between n = 1 and the lowest size stable/metastable clusters, n = 2, 2, 4, 6 for q = 1, 2, 3, 4 respectively is of similar magnitude. All adiabatic IPs have a globally decreasing trend, with an odd-even alternation consistent with the above discussion of cohesive energies. In the same line, especially high ionization potentials are observed for Au_2, Au_6, Au^+_9 , Au^+_{17}, Au^{2+}_{10} and Au^{3+}_{15} which have high stabilities.

5. Conclusion

We have here determined a complete set of total energies for Au^{q+}_n clusters for $n \leq 20$, $q \leq 4$, which allows for a thorough investigation of energetic processes involving cohesive properties, fragmentation, and ionization of gold clusters with various degrees of charge. We have investigated the stability/metastability of those clusters versus atomization and fragmentation. We have found general agreement with previous calculations or experiments available for neutral and singly charged clusters, and consistency with laser- or collision-induced dissociation experiments of doubly charged clusters, evidencing favorable fission products associated with the very stable fragment Au^{2+}_3 in the present size range. Also, Au^{2+}_{10} often appeared as a product for q = 3, 4, as well as Au^{2+}_4 for q = 4. We have also determined energy data for ionization from the ground state and confirmed with a detailed size by size study that the successive ionization potentials of gold clusters decrease rapidly away from their atomic values. While discrepancies of the present analysis (cases of fission for instance) with experimental fragmentation data are observed in some cases, one should again emphasize that the present work should be complemented by the account of barriers to dissociation, especially in the case of multiply charged clusters q = 2, 3, 4. Let us also remind here that experimental data could be affected by the specific protocols involved in cluster formation, cooling, and energy deposit. The present calculated energies are of course affected by the approximations used in the DFTB framework [35]. Nevertheless, they seem to show an overall consistency. DFTB computer efficiency is such that extensive molecular dynamics simulations of the fragmentation processes are feasible.

	q=0				q=1				q=2			q=3			q=4		
n	*lfc*	Δ_{lfc}	Δ_1	Δ_2	*lfc*	Δ_{lfc}	Δ_1	Δ_2	*lfc*	Δ_{lfc}	Δ_1	*lfc*	Δ_{lfc}	Δ_1	*lfc*	Δ_{lfc}	Δ_1
2	1+1	3.12	3.12	-	$1+1^+$	2.53	2.53	-	1^++1^+	-3.76	-	-	-	-	-	-	-
3	1+2	1.76	1.76	1.76	$2+1^+$	3.44	4.03	3.44	1^++2^+	-2.32	3.97	-	-	-	-	-	-
4	2+2	1.88	3.24	1.88	$1+3^+$	2.34	2.34	3.25	1^++3^+	-1.68	4.67	1^++3^{2+}	-5.01	-	-	-	-
5	1+4	2.82	2.82	2.95	$2+3^+$	2.59	3.37	2.59	2^++3^+	-1.17	3.04	1^++4^{2+}	-5.11	4.567	-	-	-
6	2+4	3.54	3.84	3.54	$1+5^+$	2.91	2.91	3.16	3^++3^+	-1.18	4.02	1^++5^{2+}	-4.13	4.031	$2^{2+}+4^{2+}$	-7.57	-
7	1+6	2.07	2.07	2.80	$2+5^+$	3.36	3.57	3.36	3^++4^+	-0.39	3.13	1^++6^{2+}	-3.73	4.424	$3^{2+}+4^{2+}$	-7.01	4.54
8	2+6	2.42	3.46	2.42	$1+7^+$	2.82	2.82	3.28	3^++5^+	0.15	3.92	1^++7^{2+}	-3.29	3.569	$4^{2+}+4^{2+}$	-7.25	4.42
9	1+8	2.49	2.49	2.83	$2+7^+$	3.64	3.94	3.64	3^++6^+	0.48	3.23	1^++8^{2+}	-3.21	4.002	$4^{2+}+5^{2+}$	-6.24	4.05
10	2+8	2.77	3.40	2.77	$1+9^+$	2.37	2.37	3.19	1^++9^+	1.34	4.63	1^++9^{2+}	-3.01	3.443	$4^{2+}+6^{2+}$	-5.88	4.39
11	1+10	2.71	2.71	3.00	$2+9^+$	2.76	3.50	2.76	3^++8^+	1.00	2.28	1^++10^{2+}	-3.52	4.118	$4^{2+}+7^{2+}$	-5.31	3.69
12	6+6	2.96	3.60	3.19	$1+11^+$	2.63	2.63	3.01	3^++9^+	0.84	3.78	2^++10^{2+}	-2.75	3.313	$6^{2+}+6^{2+}$	-5.31	3.94
13	1+12	2.70	2.70	3.18	$2+10^+$	2.97	3.46	2.97	3^++10^+	1.00	2.53	3^++10^{2+}	-2.90	3.880	$4^{2+}+9^{2+}$	-5.23	3.29
14	2+12	3.27	3.68	3.27	$1+13^+$	2.84	2.84	3.18	3^++11^+	1.22	3.72	4^++10^{2+}	-2.21	3.028	$4^{2+}+10^{2+}$	-6.32	3.54
15	1+14	2.77	2.77	3.33	$2+13^+$	3.23	3.50	3.23	6^++9^+	1.53	3.05	3^++12^{2+}	-1.57	4.373	$5^{2+}+10^{2+}$	-5.67	3.69
16	2+14	2.88	3.23	2.88	$1+15^+$	2.97	2.97	3.36	7^++9^+	1.34	3.38	1^++15^{2+}	-1.77	2.540	$6^{2+}+10^{2+}$	-6.09	3.60
17	1+16	3.13	3.13	3.24	$2+15^+$	3.62	3.76	3.62	8^++9^+	1.36	2.84	3^++14^{2+}	-1.43	3.858	$7^{2+}+10^{2+}$	-5.97	3.24
18	1+17	3.62	3.62	3.63	$1+17^+$	2.89	2.89	3.54	9^++9^+	1.23	3.82	3^++15^{2+}	-1.58	2.905	$8^{2+}+10^{2+}$	-5.33	4.56
19	1+18	3.28	3.28	3.78	$2+17^+$	3.42	3.64	3.42	1^++18^+	1.82	3.01	9^++10^{2+}	-1.37	3.792	$9^{2+}+10^{2+}$	-6.43	2.14
20	1+19	3.98	3.98	4.15	$1+19^+$	3.14	3.14	3.67	3^++17^+	1.67	3.52	1^++19^{2+}	-1.49	2.797	$10^{2+}+10^{2+}$	-7.11	3.95

Table II. Fragmentation energies of Au^{q+}_n clusters (in eV). *lfc* indicates the lowest energy fragmentation channels, Δ_{lfc} the corresponding energy differences $-(E^{q+}_n - E_{lfc})$, Δ_1 the energy default corresponding to a neutral monomer evaporation $-$(Eq+n $-$Eq+n$-$1 $-$ E1), Δ2 that for a neutral dimer evaporation $-(E^{q+}_n - E^{q+}_{n-2} - E_2)$ (not including barriers).

Alternatively one could also explore the fragmentation processes using entropy-based exploration such as the threshold algorithm developed by J. C. Schön [46] which allows one to feature the travel steps over neighboring barriers throughout a complex energy landscape depending on the available energy deposits in the systems, as previously done to explore the energy landscape of an anionic 20-atom gold cluster [47]. Finally, it might be interesting to extend the present study (i) to larger sizes for q = 3, 4 to reach their actual stability range, (ii) to other noble metal clusters, in particular, silver for which realistic DFTB parametrization exists [35], and (iii) to negative charge states which have also met significant interest [48, 49].

	Vertical IP (eV)				Sequential adiabatic IP (eV)			
n	Au_n^+	Au_n^{2+}	Au_n^{3+}	Au_n^{4+}	Au_n	Au_n^+	Au_n^{2+}	Au_n^{3+}
1	9.213	30.362	62.939	106.945	9.213	21.149	32.578	44.007
2	9.819	25.507	49.652	81.996	9.796	15.514	-	-
3	8.521	23.196	43.035	69.954	7.525	15.570	-	-
4	8.441	21.876	42.418	68.245	8.433	13.239	18.899	-
5	7.928	21.491	39.675	64.147	7.888	13.568	17.374	-
6	8.824	22.148	39.742	61.625	8.820	12.449	17.371	19.466
7	7.477	20.687	38.385	60.485	7.320	12.897	16.077	19.348
8	8.081	20.702	38.192	60.155	7.961	11.802	16.430	18.489
9	7.416	19.667	36.285	57.639	6.509	12.506	15.667	18.442
10	7.716	19.325	35.532	55.857	7.541	10.248	16.859	17.493
11	7.113	18.865	34.519	54.892	6.749	11.466	15.027	17.913
12	7.838	19.497	34.945	54.175	7.722	10.308	15.502	17.283
13	7.823	19.315	34.472	53.256	6.959	11.240	14.157	17.868
14	7.951	19.595	35.025	54.104	7.805	10.362	14.850	17.352
15	7.331	18.620	33.509	52.246	7.067	10.817	13.530	18.029
16	7.414	18.338	33.301	51.725	7.321	10.405	14.380	16.963
17	6.722	18.028	32.588	50.856	6.689	11.326	13.365	17.572
18	7.448	18.280	32.690	50.531	7.411	10.403	14.281	15.912
19	7.080	18.317	32.861	50.693	7.050	11.034	13.504	17.561
20	7.906	19.049	33.404	50.965	7.893	10.659	14.229	16.406

Table III. Left: Vertical ionization energies to Au^{q+}_n clusters from the Au_n global minimum. Right : Sequential adiabatic ionization potentials of Au^{q+}_n clusters .

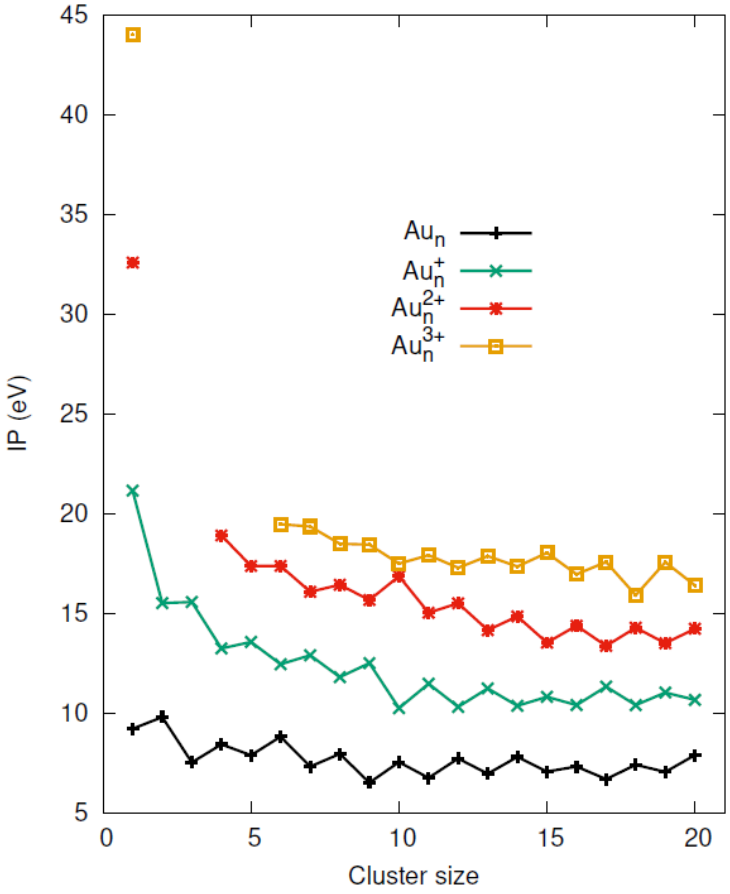

Figure 3. Sequential adiabatic ionization potentials E^{q}_{n}–$E^{(q-1)+}_{n}$ of gold clusters Au^{q+}_{n} n=2-20 with charges in the range q=0-3.

Acknowledgments

This work was granted access to the HPC resources of CALMIP supercomputing center under the allocations p0059, p18009, and p1303.

References

[1] H. Haberland, Clusters of Atoms and Molecules, edited by H. Haberland, Title Springer Series in Chemical Physics (Springer Berlin, Heidelberg, 1994).

[2] R. L. Johnston, Atomic and molecular clusters, Vol. Masters Series in Physics and Astronomy (Taylor ando and Francis, London, UK, 2002).

[3] C. Guet, P. Hobza, F. Spiegelman, and F. David, eds., Atomic clusters and nanoparticles. Les Houches Session LXXIII 2001st Edition (2001).

[4] J. A. Alonso, Structure and Properties of Atomic Nanoclusters, 2nd ed. (IMPERIAL COLLEGE PRESS, 2011).

[5] H. H¨akkinen, Chem. Soc. Rev. 37, 1847 (2008).

[6] G.-J. Kang, Z.-X. Chen, Z. Li, and X. He, J. Chem. Phys. 130, 034701 (2009).

[7] F. Baletto, J. Phys. Condens. Matter. 31, 113001 (2019).

[8] B. R. Goldsmith, J. Florian, J.-X. Liu, P. Gruene, J. T. Lyon,D. M. Rayner, A. Fielicke, M. Scheffler, and L. M. Ghiringhelli, Phys. Rev. Mater. 3, 016002 (2019).

[9] P. V. Nhat, N. T. Si, A. Fielicke, V. G. Kiselev, and M. T. Nguyen, Phys. Chem. Chem. Phys. 25, 9036 (2023).

[10] S. K. Lai and C. C. Lim, J. Comput. Chem. 42, 310 (2021).

[11] F. Spiegelman, N. Tarrat, J. Cuny, L. Dontot, E. Posenitskiy, C. Mart´ı, A. Simon, and M. Rapacioli, Advances in Physics: X5, 1710252 (2020)

[12] W. A. Saunders, Phys. Rev. Lett. 62, 1037 (1989).

[13] W. Saunders and S. Fedrigo, Chem. Phys. Lett. 156, 14 (1989).

[14] I. Rabin, C. Jackschath, and W. Schulze, Z Phys D - Atoms, Molecules and Clusters 19, 153–155 (1991).

[15] I. Rabin and W. Schulze, Chem. Phys. Lett. 201, 265 (1993).

[16] K. Hansen, A. Herlert, L. Schweikhard, and M. Vogel, Phys. Rev. A 73, 063202 (2006).

[17] A. Herlert, S. Kr¨uckeberg, L. Schweikhard, M. Vogel, and C. Walther, Journal of Electron Spectroscopy and Related Phenomena 106, 179 (2000).

[18] M. Vogel, K. Hansen, A. Herlert, and L. Schweikhard, Eur. Phys. J. D 21, 163–166 (2002).

[19] L. Schweikhard, P. Beiersdorfer, W. Bell, G. Dietrich, S. Kr¨uckeberg, K. L¨utzenkirchen, B. Obst, and J. Ziegler, Hyperfine Interact 99, 97–104 (1996).

[20] L. Schweikhard, K. Hansen, A. Herlert, M. Herr´aiz Lablanca, G. Marx, and M. Vogel, International Journal of Mass Spectrometry 219, 363 (2002).

[21] L. Schweikhard, K. Hansen, Herlert, A. M. D. Herr´aiz Lablanca, and M. Vogel, Eur. Phys. J. D 36, 179–185 (2005).

[22] J. Ziegler, G. Dietrich, S. Kr¨uckeberg, K. L¨utzenkirchen, L. Schweikhard, and C. Walther, Hyperfine Interactions 115, 171–179 (1998).

[23] J. Ziegler, G. Dietrich, S. Kr¨uckeberg, K. L¨utzenkirchen, L. Schweikhard, and C. Walther, International Journal of Mass Spectrometry 202, 47 (2000).

[24] W. A. Saunders, Phys. Rev. A 46, 7028 (1992).

[25] U. Naher, S. Bjornholm, S. Frauendorf, F. Garcias, and C. Guet, Physics Reports 285, 245 (1997).

[26] S. Kr¨uckeberg, G. Dietrich, K. L¨utzenkirchen, L. Schweikhard, and J. Ziegler, Phys. Rev. A 60, 1251 (1999).

[27] O. Echt, P. Scheier, and T. D. M¨ark, Comptes Rendus. Physique 3, 353 (2002).

[28] L. Yan, L. Cheng, and J. Yang, J. Phys. Chem. C 119, 23274 (2015).

[29] R. Pis Diez and J. A. Alonso, Journal of Molecular Structure: THEOCHEM 639, 203 (2003).

[30] G. Ortiz and P. Ballone, Phys. Rev. B 44, 5881 (1991).

[31] A. A. A. Attia, A. M. V. Brˆanzanic, A. Mu˜noz Castro, A. Lupan, and R. B. King, Phys. Chem. Chem. Phys. 21, 17779 (2019).

[32] B. Molina, J. Soto, and A. Calles, Eur. Phys. J. D 51, 225 (2009).

[33] P. M. Petrar, M. B. S´arosi, and R. B. King, J. Phys. Chem. Letters 3, 3335 (2012).

[34] M. Barysz and P. Pyykk¨o, Chemical Physics Letters 325, 225 (2000).

[35] N. Tarrat, M. Rapacioli, J. Cuny, J. Morillo, J.-L. Heully, and F. Spiegelman, Comput. Theor. Chem. 1107, 102 (2017).

[36] K. Balasubramanian and P. Feng, Chemical Physics Letters 159, 452 (1989).

[37] B. Assadollahzadeh and P. Schwerdtfeger, J. Chem. Phys. 131, 064306 (2009).

[38] E. M. Fern´andez, J. M. Soler, I. L. Garz´on, and L. C. Balb´as, Phys. Rev. B 70, 165403 (2004).

[39] M. Gao, A. Lyalin, M. Takagi, S. Maeda, and T. Taketsugu, J. Phys. Chem. C 119, 11120 (2015).

[40] A. V. Walker, J. Chem. Phys. 122, 094310 (2005).

[41] P. Ferrari and E. Janssens, Molecules 26 (2021).

[42] W. A. Saunders, Phys. Rev. Lett. 64, 3046 (1990).

[43] M. Vogel, K. Hansen, A. Herlert, and L. Schweikhard, Eur. Phys. J. D 16, 73–76 (2001).

[44] M. Vogel, A. Herlert, and L. Schweikhard, Journal of the American Society for Mass Spectrometry 14, 614 (2003).

[45] W. Schulze, B. Winter, and I. Goldenfeld, Phys. Rev. B 38, 12937 (1988).

[46] S. Neelamraju, C. Oligschleger, and J. C. Sch¨on, J. Chem. Phys. 147 (2017).

[47] M. Rapacioli, C. J. Sch¨on, and N. Tarrat, Theor. Chem. Acc. 140, 85 (2021).

[48] A. Herlert, S. Kr¨uckeberg, L. Schweikhard, M. Vogel, and C. Walther, Physica Scripta 1999, 200 (1999).